Pergamon

Int. J. Heat Mass Transfer. Vol. 41, Nos 4–5, pp. 757–767, 1998

Printed in Great Britain
0017–9310/98 $19.00+0.00

PII: S0017–9310(97)00182–8

Homogeneous nucleation and macroscopic growth of gas bubble in organic solutions

HO-YOUNG KWAK
Mechanical Engineering Department, Chung-Ang University, Seoul 156-756, Korea

and

YONG W. KIM
Allied Signal Inc., 111S 34th Street, Phoenix, AZ 85072-2181, U.S.A.

(*Received* 24 *November* 1996 *and in final form* 12 *May* 1997)

Abstract—This work concerns the spontaneous gas bubble nucleation after rapid decompression in organic solution initially saturated with dissolved gas and the subsequent bubble growth to macroscopic size. The decompression limit for gas bubble formation was obtained from the stability condition of the critical cluster of dissolved gas molecules. This work also clarifies how the critical cluster grows to the critical size bubble, the first object which is separated from liquid molecules by interface. Further growing of this critical size bubble by diffusion process was treated by an integral method for the concentration boundary layer thickness. The calculation values of the amount of decompression for the homogeneous gas bubble formation in organic solutions and the time required for the birth of macroscopic bubble size are in reasonable agreement with experimental results. © 1997 Elsevier Science Ltd.

INTRODUCTION

Spontaneous bubble formations occur after a gas–liquid solution initially saturated with dissolved gas molecules is rapidly decompressed. Such phenomenon is observed in many industrial examples such as "vacuum" degassing of molten metals [1] and the manufacture of foamed materials [2] and cellular polymers [3]. It is also known to be the major cause of caisson disease in which case the gas bubble nucleation occurs within blood vessels and tissues due to excessive rate of decompression [4]. The subject of bubble nucleation, or the ensuing rate of gas evolution from the liquid thus deserves a considerable interest in a broad range of science and technology.

Hemmingsen [5, 6] carried out an extensive experimental study on gas nucleation in various gas–water solutions caused by rapid decompression and observed that the amount of decompression for bubble formation in water solution varies with solute gas species. Kaddah [1] studied the problem of CO degassing in molten iron at 1600°C and found that CO bubble formation depends crucially on the oxygen activity in the solution. Experiments on gas bubble formation in elastomer were conducted by Gent [2]. Also experimental study on the nitrogen bubble nucleation in various organic solutions was performed by Hong [7].

Theoretical considerations on bubble nucleation by dissolved gas in liquids are rather limited as compared with the case of bubble nucleation by vapor molecules (boiling phenomena) [8]. A gas bubble nucleation model based on molecular interactions in gas–liquid solutions was proposed by Kwak and Panton [9]. In their model it is assumed that the surface energy needed for bubble formation is equal to the translational motion of gas molecules which is lost during the dissolution process [10]. The model also postulates the concept of the critical cluster which is embedded in liquid molecules; once the cluster reaches the critical size it grows further by kinetics without any hindrance. On the other hand, macroscopic growing of gas bubble without any specification of the initial size was studied by many researchers, such as Scriven [11], Epstein and Plesset [12], and Rosner and Epstein [13]. Recently, Arefmanesh *et al.* [14] developed an accurate numerical technique based on potential theory to study diffusion-induced bubble growth in viscous liquids. However, no work was attempted to grow the critical size bubble forms from the cluster and this bubble grows to a macroscopic size bubble.

Present works bridge the gap between bubble nucleation theory and the available mathematical treatment on the diffusion controlled bubble growth, thereby the birth and subsequent bubble growth of a gas bubble immediately after decompression can both be accounted for. For this purpose, the gas bubble nucleation model by Kwak and Panton [9] is adjusted to the case of organic solutions by suitable molecular volume transformation [15]. The resulting size of the critical cluster obtained by the stability condition of the cluster provides the amount of decompression for

NOMENCLATURE

A_n	surface area of n-mer cluster
c	solute concentration
D	gas diffusion coefficient in solution
D_g	rate of molecules striking on the surface of n-mer cluster
f_L	lost degree of freedom of dissolved gas molecules
F_n	free energy need to form n-mer cluster
J_n	nucleation rate of n-mer cluster per unit volume
k	Boltzmann constant
K_H	Henry constant
m_g	mass of dissolved gas molecule
$\dot{m}''$	mass flux
n	number of molecules in a cluster or in a bubble
N_g	number of dissolved gas molecules per unit volume
N_l	number density of solution
P_i	initial equilibrium pressure with gas
P_g	pressure inside bubble
P_r	concentration profile
P_∞	ambient pressure
r	distance from bubble center
r_n	radius of n-mer cluster
R	radius of bubble
R_g	gas constant
R_0	initial bubble radius
T	liquid temperature
T_f	melting temperature of liquid
v	radial velocity in liquid
$\bar{V}$	average speed of molecule in liquid
v_g	molecular volume of dissolved gas
v_N	specific volume of liquid
Z_{fg}	Zeldovich nonequilibrium factor.

Greek symbols

β_g	accommodation coefficient
Γ	Gibbs absorption at the interface
δ	concentration boundary layer thickness
ΔH_{vap}	enthalpy of evaporation
ΔH_f	enthalpy of fusion
ρ	density of solution
ρ_g	gas density inside bubble
σ	interfacial tension
σ_0	interfacial tension with infinite curvature
σ_{LJ}	Lennard–Jones parameter.

Subscripts

c	critical size cluster
0	initial condition
w	wall
chem	chemical equilibrium
∞	property evaluation far from the bubble center.

bubble nucleation. Also, it is assumed that kinetic growth continues until the number of molecules inside the cluster is enough to become the critical size bubble, which is the very first object separated from the liquid molecules by the interface. The growth of this bubble is assumed to be due to concentration defect through the interface by the diffusion process. The concentration boundary layer thickness as a means of the driving force for the diffusion process is calculated by the integral method developed by Rosner and Epstein [13] with some modification.

The calculation values of the amount of decompression for the homogeneous gas bubble formation in organic solutions and the time required for the birth of macroscopic size bubble in solutions are in reasonable agreement with experimental results.

GAS BUBBLE NUCLEATION

Consider a liquid–gas solution saturated with gas pressure P_i at temperature T. As a result of a pressure reduction, an ambient pressure, P_∞ the dissolved gases become supersaturated. In this metastable state, aggregation of the dissolved gas molecules into clusters may be imagined. The change in free energy of the cluster molecules plus the surface energy as postulated is the free energy required to form an n-mer cluster [9]. This is

$$F_n = -(P_i - P_\infty)nv_g + \frac{f_L}{2}kTn^{2/3}. \quad (1)$$

The "lost degree-of-freedom", f_L, during the dissolution process represents the solvent–solute interaction effect, which is given by

$$f_L/3 = \widehat{v_g}/v_g \quad (2)$$

where $\widehat{v_g}$ is the molecular volume which restrains all the translational motion of the gas molecule. The condition for a minimum with respect to n in the free energy of formation is found from eqn (1) to be

$$(P_i - P_\infty)n^{1/3} = \frac{f_L}{3}\frac{kT}{v_g}. \quad (3)$$

With the following transformed molecular volume of the dissolved gas and the corresponding number of molecules in the cluster [15] such as

$$v_g = (f_L/3)^{3/2} v'_g \tag{4-1}$$

$$n = (3/f_L)^{3/2} n' \tag{4-2}$$

the above stability condition for the cluster becomes a standard form [9]. It is

$$(P_i - P_\infty) n'^{1/3} = \frac{kT}{v'_g}. \tag{3}'$$

The corresponding free energy for the formation of the n_c-mer cluster may be obtained by replacing n' as n_c

$$\frac{F_{nc}}{kT} = \frac{1}{2} n_c^{2/3}. \tag{5}$$

The growth of a cluster in the supersaturated solution depends on kinetic events within the liquid. At present, the kinetic theory of the dissolved gas molecules in solution is not yet clearly understood. However, assuming that the mean velocity of the dissolved gas molecules and the number of activated gas molecules per unit volume in solution depend on solution properties, one may get the nucleation rate of the n_c-mer cluster by dissolved gases [16].

$$J_{nc} = Z_{fg} D_g N_g \exp(-\tfrac{1}{2} n_c^{2/3}). \tag{6}$$

Here D_g is the rate of molecules strike on the surface area of the cluster and Z_{fg} is the Zeldovich non-equilibrium factor such as

$$Z_{fg} = \left[-\frac{1}{2\pi kT} \left(\frac{\partial^2 F_n}{\partial n^2} \right)_{n=n_c} \right] \tag{7}$$

$$D_g = \frac{\beta_g}{4} \bar{V} \bar{N}_g A_n. \tag{8}$$

In eqn (8), $\bar{V}$ is the average speed of the gas molecules within the solution, $\bar{N}_g$ is the number of activated gas molecules per unit volume and A_n is the n-mer cluster surface area given as $A_n = 4\pi r_n^2 = 4\pi r_g^2 n^{2/3}$. The average speed of dissolved gas molecules and the activated gas molecules per unit volume may be estimated as [17]

$$\bar{V} = \left(\frac{8kT}{\pi m_g} \right)^{1/2} \exp\left[-\frac{\Delta H_f}{R_g T_f} \right] \tag{9}$$

$$\bar{N}_g = N_g \exp\left[-\frac{\Delta H_{vap}}{R_g T} \right]. \tag{10}$$

The parameters in the exponential terms are solution properties; ΔH_{vap} and ΔH_f are the enthalpies for the evaporation and the freezing of the solution, respectively, and T_f is the melting temperature of the solution. With the expression for the minimum free energy of the clustering process given as eqn (5) and using eqns (7)–(10), the nucleation rate, J_{nc} for the formation of the critical cluster is obtained. It is

$$J_{nc} = \frac{N_g}{\sqrt{6\pi}} \left(\frac{kT}{2\pi m_g} \right)^{1/2} 4\pi \left(\frac{3v_g}{4\pi} \right)^{2/3} \beta_g (f_L/3)^{3/2} \times \exp\left[-\frac{\Delta H_{vap}}{R_g T} - \frac{\Delta H_f}{R_g T_f} \right] N_g \exp\left[-\frac{1}{2} n_c^{2/3} \right]. \tag{6}'$$

From eqn (6)′, one may estimate the number of molecules of the critical cluster by substituting a suitable value for J_{nc}. It is assumed that $J_{nc} = 10^6$ nuclei cm^{-3} corresponds to the massive bubble formation, while $J_{nc} = 1$ corresponds to the threshold of bubble formation. Given the value of n_c the amount of decompression is calculated from eqn (3). In this calculation, the partial molar volume of gas in organic solutions, which is needed for obtaining the effective molecular volume of dissolved gas was estimated using the correlation of Lyckman *et al.* [18]. Also, the dissolved gas molecular volume which restrains all the translational motion of the gas molecule was estimated using the Lennard–Jones parameter σ_{LJ} [19] in the relation,

$$\widehat{v_g} = \frac{\pi\sqrt{2}}{6} \sigma_{LJ}^3. \tag{11}$$

The effective volume that a single molecule occupies in water solution is a well defined physical quantity [20]. However, one cannot easily estimate the molecular volume of dissolved gases in large molecule solutions such as organic or polymeric ones [3], which in turn provides less accurate decompression amount for bubble formation. Another mechanism, in addition to the solute–solvent interactions, should be included to encounter the bubble formation in a melt system with high surface tension and low vapor pressure [21].

A MODEL OF TRANSITION FROM THE CRITICAL CLUSTER TO THE CRITICAL SIZE BUBBLE

The concept of the critical cluster postulated by the Kwak–Panton bubble nucleation model has the following physical implication. The clustering process is the first step in forming a gas bubble within a liquid after rapid decompression, in which numerous dissolved gas molecules group together to form a critical cluster. It is further assumed that once the critical cluster, corresponding to given conditions, is formed, its growing to a macroscopic gas bubble is guaranteed. Therefore, it can be said that the critical cluster quantitatively defined by the bubble nucleation model [9] serve as "seeds" for the subsequent formation of the critical size bubble, which is the starting point of classical nucleation theory [22]. In other words, no additional energy is needed for the formation of the critical size bubble from the critical cluster. One may imagine that the cluster molecules closely packed with surrounding liquid molecules will behave quite differently from those constituting a gas bubble, which has a clear interface [9].

First, we consider a gas bubble composed of n mol-

ecules of ideal gas, which is in mechanical equilibrium with the surrounding liquid. Then the following relations can be shown to hold for an arbitrary bubble radius R.

$$P_g \tfrac{4}{3}\pi R^3 = nkT \tag{12}$$

$$P_g - P_\infty = \frac{2\sigma}{R} \tag{13}$$

where

$$\sigma = \sigma_0 \Big/ \left[1 - \frac{2\Gamma v_N}{R}\right]. \tag{14}$$

Eqn (14) is the expression for the surface tension correction depending on the radius of curvature [23] in which Γ is the Gibbs absorption at the interface and σ_0 is the measured surface tension value at temperature T. Note that more surface tension is applied to the smaller size bubble, which is different from a droplet system.

If such a bubble exists in a supersaturated liquid–gas solution, the bubble will grow by means of molecular diffusion. The diffusion process can be described by the Fick's law, where the mass flux into the bubble is depending on the concentration gradient near the bubble boundary. The concentration gradient is, in turn, depending on the variation of the concentration at the gas–liquid interface. In the present work, it is assumed that the dissolved gas weight fraction at the bubble wall is related to the pressure inside the bubble according to Henry's law such that

$$c_w = \frac{m_g N_l}{\rho}\frac{P_g}{K_H}. \tag{15}$$

If the initial pressure before decompression is P_i, the solute supersaturation concentration, c_∞ can be written as

$$c_\infty = \frac{m_g N_l}{\rho}\frac{P_i}{K_H}. \tag{16}$$

One notes that in order for the diffusion process to take place toward the bubble growth, $c_w < c_\infty$ must hold and, hence, $P_g < P_i$ from eqns (15) and (16). Therefore, any bubble formed from the critical cluster must satisfy $P_g = P_i$. We tentatively assume the condition, $c_w = c_\infty$ as a definition of the chemical equilibrium of the system. Then, by setting $P_g = P_i$, the number of molecules forming the bubble in mechanical and chemical equilibrium can be readily computed from eqns (12) and (13). The resulting value of n_{chem}, the number of molecules in the bubble which is in the chemical and mechanical equilibrium conditions, turns out to be much higher than that in the critical cluster, n_c. This means that the pressure of the bubble having the same number of molecules as the critical cluster is much higher than that of the bubble corresponding to the chemical and mechanical equilibrium conditions, the critical size bubble. It is obvious that such a bubble will shrink to disappear as a result of counter diffusion, since $c_w > c_\infty$. Thus, no bubble which has a smaller number of molecules than n_{chem} can survive as a bubble. Further, this kind of bubble cannot overcome the interfacial tension, as can be seen from eqns (12) and (13). Therefore, the only plausible physical reasoning will be to assume that the critical cluster continues to grow by molecular kinetics until the transition from the cluster to the critical size bubble finally takes place as the number of molecules forming the cluster passes that required for the critical size bubble [24]. Such reasoning is always possible in view of the fact that the clusters are subject to continuous molecular collisions and that different sizes of cluster are considered as different species of molecules [25].

The kinetic controlled growth of the critical cluster resulting from molecular collisions can be estimated from the previous nucleation kinetics, i.e. the rate of molecular collision on the n-mer cluster is given by eqn (8).

$$\frac{dn}{dt} = D_g = \beta_g \bar{V} \bar{N}_g r_g n^{2/3}. \tag{17}$$

Separating the variables and integrating over arbitrary n and t gives approximately

$$n_{chem} = [3\beta_g \pi \bar{V} \bar{N}_g r_g t]^3. \tag{18}$$

With known values of n_{chem}, the time lag needed to reach the cluster with n_{chem} molecules can be directly computed from eqn (18). The results of the calculation are typically in ms range which can be safely neglected for the characteristic time of macroscopic bubble growth. Practically, the numerical calculation for diffusional growth was started with the number molecules inside the bubble, $n_{chem} + 10$.

MACROSCOPIC GROWING OF A BUBBLE

Basic analysis for diffusion controlled bubble growth

Once the transition from a cluster to a gas bubble takes place, the subsequent diffusion controlled bubble growth can be analyzed by available mathematical treatment. Theoretically, the bubble which is in mechanical and chemical equilibrium will not grow. However, a small number of molecules added by molecular collisions to the critical size bubble are enough to trigger the bubble to grow by a diffusion process. This is why we start the diffusional growth with $n_{chem} + 10$. The present analysis employs the following assumptions for simplification:

(i) the bubble is solely composed of dissolved gas molecules and the gas inside behaves as an ideal gas;

(ii) the bubble remains spherical at all times and any translational motions caused by buoyancy effects within the surrounding liquid are neglected;

(iii) the pressure inside the bubble is always in mechanical equilibrium with that of the surrounding liquid by the interfacial tension. Therefore, the instan-

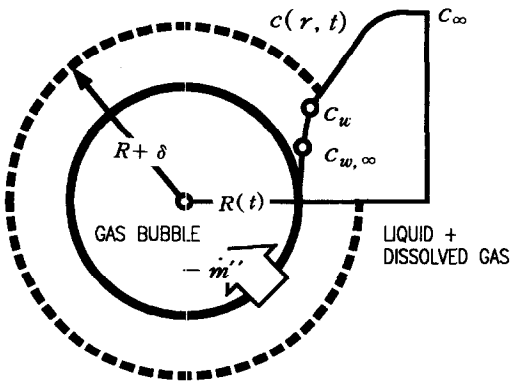

Fig. 1. Physio-chemical model of spherical bubble growth in a supersaturated liquid configuration.

taneous pressure differences by inertial and viscous effects are neglected;

(iv) the temperature of the system and property values remain constant during the entire process.

Figure 1 gives the configuration of the present model for an arbitrary gas bubble within a gas–liquid solution. The mass balance across the gas–liquid interface provides the following relation:

$$4\pi R^2 \dot{m}'' = -\frac{\mathrm{d}}{\mathrm{d}t}\left(\frac{4}{3}\pi\rho_g R^3\right) \tag{19}$$

where $\dot{m}''$ is the interfacial mass flux and the negative sign is due to the choice of present coordinate system. In view of assumptions (i) and (iii) and from eqns (12) and (13), the time dependent gas density $\rho_g(t)$ can be shown to be related to the gas pressure $P_g(t)$ as follows:

$$\rho_g(t) = \frac{P_g}{R_g T} = \frac{1}{R_g T}\left[P_\infty + \frac{2\sigma_0}{R\left(1-\dfrac{2\Gamma v_N}{R}\right)}\right] \tag{20}$$

then eqn (19) can be rewritten for $\dot{m}''$ as

$$-\dot{m}'' = \left[\rho_\infty + \frac{2\sigma_0}{R_g T}\frac{2R-6\Gamma v_N}{3(R-2\Gamma v_N)^2}\right]\frac{\mathrm{d}R}{\mathrm{d}t}. \tag{21}$$

The Fick's law relates the mass transfer rate to the concentration gradient near the bubble boundary such that

$$-\dot{m}'' = \frac{D\rho}{1-c_w}\left(\frac{\partial c}{\partial r}\right)_{r=R} \tag{22}$$

where c is the dissolved gas weight fraction as defined in eqn (15). The governing conservation for the solute concentration in the spherical coordinate system can be written as

$$\rho\frac{\partial c}{\partial t} + \rho v\frac{\partial c}{\partial r} = \rho\frac{D}{r^2}\frac{\partial}{\partial r}\left(r^2\frac{\partial c}{\partial r}\right); \quad r \geqslant R(t). \tag{23}$$

The concentration satisfies the following initial and boundary conditions:

$$c(r, t=0) = c(r=\infty, t) = c_\infty. \tag{24}$$

With these conditions given in eqn (24), Epstein and Plesset [12] solved the mass conservation equation, eqn (23), without radial convection term, which yields an analytical solution.

For an incompressible fluid, the velocity in fluid $v(r, t)$ is related to $v(R)$ on the bubble boundary through the continuity such that

$$vr^2 = v(R)R^2; \quad r \geqslant R(t). \tag{25}$$

Across the interface at $r = R(t)$, the overall mass conservation also gives

$$\dot{m}'' = \rho[v(R) - \dot{R}] \tag{26}$$

where $\dot{R}$ is the instantaneous radial velocity of the bubble wall caused by the inertial effects. However, the radial velocity contributed from the momentum equation is neglected in view of assumption (iii). Only the convection due to diffusional growth is considered in this analysis.

The basic objective of the present analysis is to find the radius–time history of bubble growth corresponding to the time dependent concentration on the bubble wall, $c_w(t)$, which satisfies the above conservation equation and initial and boundary conditions.

Reformulation of the problem using an integral method

The integral method, which can be classified as one member of weighted residual methods, is particularly well suited to the present problem where the dependent variable c on the bubble wall is time-dependent. The present analysis is patterned after the work by Rosner and Epstein [13] with some modification. The underlying idea in applying the method is to assume a suitable functional form for the radius dependence of the concentration field which includes an undetermined function of time. For the present problem, the undetermined function is just the solute concentration boundary layer thickness δ. This arbitrary function is then introduced into the governing solute conservation equation with a reasonable assumption for the concentration profile. This boundary layer thickness, which represents the degree of concentration defect at the bubble interface, is a crucial factor for diffusion process. Introducing suitable interfacial kinetics [13], the concentration boundary layer thickness was eliminated to obtain the time rate change of bubble radius. In this study, however, the boundary layer thickness was calculated directly by solving the cubic equation for δ obtained from the solute conservation equation with a polynomial profile. This method turned out to be very successful in studying the heat transfer for single bubble motion in ultrasonic field [26, 27]. Also note that such polynomial profiles turn out to be reasonable approxi-

mations for the initial stage of bubble growth [14] as well as for the later stage of diffusional growth as can be confirmed in this study.

The governing conservation equation can be written with the aid of eqns (25) and (26) as follows:

$$r^2\frac{\partial}{\partial t}(c_\infty - c) = -\left(\dot{R}+\frac{\dot{m}''}{\rho}\right)R^2\frac{\partial}{\partial r}(c_\infty - c) + D\frac{\partial}{\partial r}\left[r^2\frac{\partial}{\partial r}(c_\infty - c)\right]. \quad (27)$$

Integrating from $r = R$ to $r = R+\delta$ and using the boundary conditions, eqn (27) reduces to

$$\frac{\mathrm{d}}{\mathrm{d}t}\int_R^{R+\delta} r^2(c_\infty - c)\,\mathrm{d}r = (1-c_\infty)\frac{\mathrm{d}}{\mathrm{d}t}\left(\frac{\rho_g}{\rho}\frac{R^3}{3}\right). \quad (28)$$

In deriving the above equation, the terms related to the bubble wall motion due to inertia effect are canceled out. Since ρ_g is related to P_g through the ideal gas law and R is solely time dependent, eqn (28) can be integrated with respect to t such that

$$\int_R^{R+\delta} r^2\frac{c_\infty - c}{c_\infty - c_w}\mathrm{d}r = \frac{1-c_\infty}{c_\infty - c_w}\frac{\rho_g R^3 - \rho_{g,0}R_0^3}{3\rho} \quad (29)$$

where subscript "0" denotes the initial condition. Since c_w is solute concentration at bubble wall. Rosner and Epstein [13] consider the following profile for the normalized solute concentration:

$$\frac{c_\infty - c}{c_\infty - c_w} = \begin{cases} P_r(\xi) & \text{if } R \leqslant r \leqslant R+\delta \\ 0 & \text{if } r \geqslant R+\delta \end{cases} \quad (30)$$

where

$$\xi = \frac{r-R}{\delta}$$

and the concentration profile, $P_r(\xi)$, is given by

$$P_r(\xi) = (1-\xi)^2. \quad (31)$$

This choice of the solute concentration profile satisfies that

$$P_r(0) = 1 \quad \text{and} \quad P_r(1) = 0 \quad (32)$$

and also that

$$\left.\frac{\mathrm{d}P_r(\xi)}{\mathrm{d}\xi}\right|_{\xi=1} = 0.$$

Then it can be shown that eqn (29) becomes

$$\left[\frac{1}{10}\left(\frac{\delta}{R}\right)^3 + \frac{1}{2}\left(\frac{\delta}{R}\right)^2 + \left(\frac{\delta}{R}\right)\right] = \left(\frac{1-c_\infty}{c_\infty - c_w}\right) \times \frac{\left[\left(\rho_\infty + \frac{2\sigma_0}{R_g T(R-a)}\right)R^3 - \left(\rho_\infty + \frac{2\sigma_0}{R_g T(R_0-a)}\right)R_0^3\right]}{\rho R^3} \quad (33)$$

where

$$a = 2\Gamma v_N.$$

A different concentration profile may lead to a quadratic equation for δ [28], which is readily solvable. However, this concentration profile yields an integral equation for the bubble radius $R(t)$, which needs an assumed value of $R(t)$ and requires repeated iteration until a satisfactory convergence for solving it. With the above choice of profile, the mass flux given by eqn (22) can be written as

$$\dot{m}'' = \left(\frac{c_\infty - c_w}{1-c_w}\right)\frac{D\rho}{\delta}\left(\frac{\mathrm{d}P_r}{\mathrm{d}\xi}\right)_{\xi=0} = -\frac{2D\rho}{\delta}\left(\frac{c_\infty - c_w}{1-c_w}\right). \quad (34)$$

The mass transfer rate is also given by eqn (21). Then eliminate $\dot{m}''$ from eqns (21) and (34) to obtain

$$\frac{\mathrm{d}R}{\mathrm{d}t} = \frac{2D\rho\left(\frac{c_\infty - c_w}{1-c_w}\right)}{R\left[\rho_\infty + \frac{2\sigma_0(2R-3a)}{3R_g T(R-a)^2}\right]\left(\frac{\delta}{R}\right)}. \quad (35)$$

With $c_w(t)$ related to $R(t)$ through eqns (15) and (20), eqns (33) and (35) constitute a system of ordinary differential equations for $R(t)$. Due to the complex algebraic terms on the left-hand side of eqn (33), this system cannot be readily treated analytically. One may note that Rosner and Epstein [13] made a thin boundary layer assumption such that $\delta/R \ll 1$, whereby only the first-order term on the LHS of eqn (33) was retained. With this assumption, eqn (35) becomes a separable equation for bubble radius, R w.r.t. the solute concentration terms. However, as will be discussed in a later section, such assumption is applicable only for a relatively large size bubble. Eqn (35) represents the bubble growth due to the concentration defect near the bubble wall as is assumed. However, in general, the bubble wall motion is determined by the inertia force [29].

The solution of eqns (33) and (35) is then approached by introducing suitable nondimensional variables such as

$$\varepsilon = R/R_0 \quad (36a)$$

$$A = a/R_0 \quad (36b)$$

$$x = t/t_r \quad (36c)$$

$$\bar{z} = \frac{2\sigma_0}{\rho_\infty R_0 R_g T} = \frac{2\sigma_0}{R_0 P_\infty} \quad (36d)$$

$$F = c_\infty / c_{w,\infty} \quad (36e)$$

where

$$t_r = \frac{R_0^2}{2D}\frac{\rho_\infty}{\rho} \quad (36f)$$

and

$$c_{w,\infty} = \frac{m_g N_1}{\rho}\frac{P_\infty}{K_H}. \quad (36g)$$

Using these nondimensional variables, eqns (33) and (35) can be rewritten as

$$\left[\frac{1}{10}\left(\frac{\delta}{R}\right)^3+\frac{1}{2}\left(\frac{\delta}{R}\right)^2+\frac{\delta}{R}\right]=\frac{(1-Fc_{w,\infty})}{c_{w,\infty}\dfrac{\rho}{\rho_\infty}\left(F-1-\dfrac{\bar{z}}{\varepsilon-A}\right)}\cdot\left(\frac{\left(1+\dfrac{\bar{z}}{\varepsilon-A}\right)\varepsilon^3-\left(1+\dfrac{\bar{z}}{1-A}\right)}{\varepsilon^3}\right) \quad (33)'$$

and

$$\varepsilon\frac{d\varepsilon}{dx}=\frac{c_{w,\infty}}{\left(\dfrac{\delta}{R}\right)}\left[\frac{F-1-\dfrac{\bar{z}}{\varepsilon-A}}{1-c_{w,\infty}\left(1+\dfrac{\bar{z}}{\varepsilon-A}\right)}\right]\cdot\left[\frac{1}{1+\dfrac{\bar{z}}{3}\dfrac{(2\varepsilon-3A)}{(\varepsilon-A)^2}}\right] \quad (35)'$$

A numerical calculation procedure for solving the above equations is as follows. First, for a given time step, the boundary layer thickness ratio, δ/R, is calculated from eqn (33)′ using the Newton's method. Next, the resulting value of δ/R at a given radius of R is introduced into eqn (35)′ and then $R(t)$ for the next time step is calculated using the fourth-order Runge–Kutta numerical integration scheme. The above procedure is repeated up to the desired time step.

RESULTS AND DISCUSSIONS

Table 1 gives the calculated results for nitrogen bubble formation in various organic solutions and comparisons with experimental data by Hong [7]. In addition, calculation values by the classical nucleation theory are listed. As shown in this table, the decompression values calculated are in reasonable agreement with experimental results, while the classical theory overestimates the events in general. Experimental results showed that the surface tension dependence on the bubble formation is not conclusive, for example, the decompression value for nitrogen bubble formation in benzene is less than that in ethanol. Comparing these calculated values with the experimental results, the prediction in benzene is too high, while those in chloroform and hexane are too low. The main difficulty in predicting the decompression limit for gas bubble formation in organic solutions is that we cannot estimate the molecular volume occupied by dissolved gas molecules properly at present. Also note that the decompression amount obtained by Hong [7] may be low; for the threshold nitrogen bubble formation in water, the decompression value obtained by Hong (120 atm) is less than that by Hemmingsen (160 atm).

Two cases of organic solutions: benzene and carbon tetrachloride are considered for the present example calculation of macroscopic bubble growth. The dissolved gas is nitrogen for both cases. The calculation result of radius–time history of gas bubble from the critical size is shown in Figs 2 and 3. The initial radius, R_0, and the corresponding number of molecules inside the critical size bubble, n_{chem}, are also given in the figures. The two graphs show a similar pattern of growing: i.e. a slow development at the beginning followed by a rapid growth leading to the typical diffusional one ($R^2 \propto t$) which has also been verified by an experiment on the bubble growth during rapid decompression in liquid [28]. It should be noted that the bubble growth is dominated by the well known parabolic growth because the initial stage is rather short as can be seen in this figure. The trend of relatively large variations during the initial stage of growth is mainly due to the behavior of the boundary layer thickness. Table 2 gives a list of calculation

Table 1. The decompression limit of nitrogen gas in various organic solutions at 20°C (the surface tension data were obtained from *CRC Handbook of Chemistry and Physics*, CRC Press Inc., 1979)

Liquid (surface tension at 20°C; dyne cm^{-1})	Present theory		Classical theory	Experiment [7] (atm) (massive bubble formation)
	J_{nc} = 1 (atm)	J_{nc} = 10^6 (atm)	J = 1 (atm)	
Methanol (22.61)	86	108	250	90
Ethanol (22.75)	80	105	252	80
Chloroform (27.14)	45	57	330	70
Carbon tetrachloride (26.65)	30	48	326	53
Benzene (28.85)	49	59	361	35
n-Hexane (18.43)	31	41	184	56

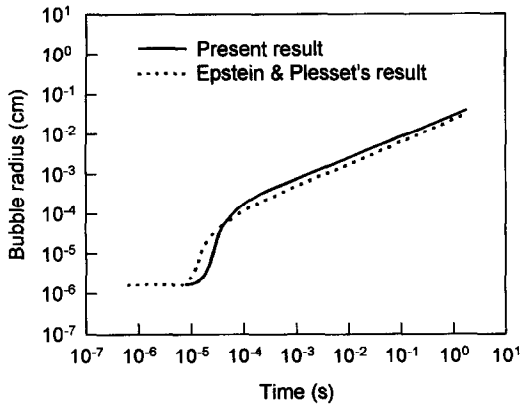

Fig. 2. A comparison between calculation results by present model and Plesset's solution for bubble growth in benzene–nitrogen solution; $R_0 = 0.171 \times 10^{-5}$ cm, $n_{chem} = 18\,268$.

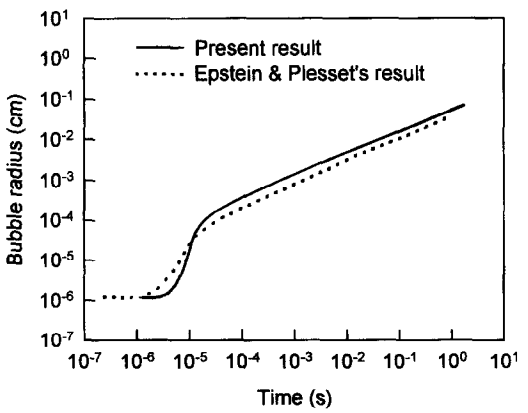

Fig. 3. A comparison between calculation results by present model and Plesset's solution for bubble growth in carbon tetrachloride–nitrogen solution; $R_0 = 0.106 \times 10^{-5}$ cm, $n_{chem} = 6535$.

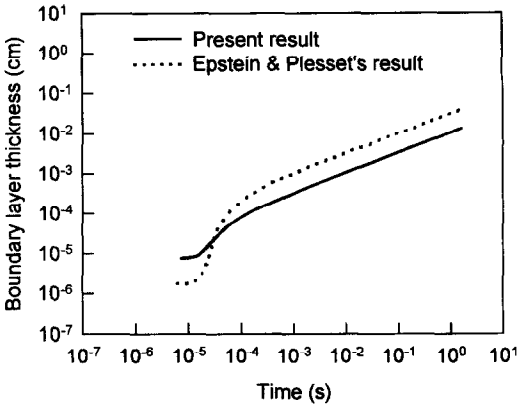

Fig. 4. Boundary layer thickness δ as function of time t in benzene–nitrogen solution.

results for the case of benzene–nitrogen system, in which the behavior of boundary layer thickness is given in detail. The value of δ/R is very large at the initial stage of bubble growing: however, the value is nearly constant for later stages as expected.

For comparisons, the calculation results by the classical work of Epstein and Plesset [12] are also shown in Figs 2 and 3. The analytical result based on steady-state concentration defect neglecting the convection term leads to the constant value of relative boundary layer thickness asymptotically. As shown in these figures, Epstein and Plesset's work overestimates the initial bubble growth and the trend is reversed such that the subsequent growing is greatly underestimated compared to the present work. However, a similar overall-trend has been obtained from both works. The corresponding variations of the boundary layer thickness shown in Fig. 4 well describes the discrepancy between the two analyses. As expected, an exact reverse trend is observed, which clarifies the importance of the boundary layer thickness as the major

Table 2. Bubble radius and boundary layer thickness as function of time; a list of calculation for benzene–nitrogen solution

Time (s)	Bubble radius (cm)	Boundary layer thickness (cm)	δ/R
0.195×10^{-5}	0.171×10^{-5}	0.788×10^{-5}	4.610
0.135×10^{-4}	0.173×10^{-5}	0.786×10^{-5}	4.546
0.212×10^{-4}	0.272×10^{-5}	0.975×10^{-5}	3.583
0.322×10^{-4}	0.210×10^{-4}	0.204×10^{-4}	0.790
0.438×10^{-4}	0.698×10^{-4}	0.364×10^{-4}	0.521
0.734×10^{-4}	0.135×10^{-3}	0.566×10^{-4}	0.419
0.110×10^{-3}	0.209×10^{-3}	0.794×10^{-4}	0.380
0.250×10^{-3}	0.400×10^{-3}	0.138×10^{-3}	0.345
0.845×10^{-3}	0.853×10^{-3}	0.276×10^{-3}	0.324
0.164×10^{-2}	0.124×10^{-2}	0.401×10^{-3}	0.323
0.744×10^{-2}	0.276×10^{-2}	0.861×10^{-2}	0.312
0.280×10^{-1}	0.545×10^{-2}	0.168×10^{-2}	0.309
0.217	0.154×10^{-1}	0.473×10^{-2}	0.307
0.434	0.207×10^{-1}	0.666×10^{-2}	0.307

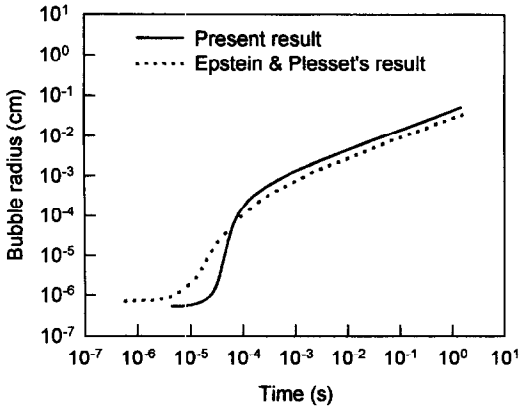

Fig. 5. A comparison between calculation results by present model and Plesset's solution for bubble growth in water–nitrogen solution; $R_0 = 0.781 \times 10^{-6}$ cm, $n_{chem} = 9521$.

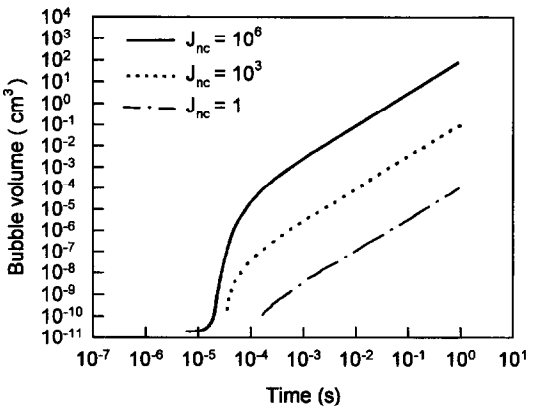

Fig. 6. The volume occupied by gas bubble per unit volume depending on the nucleation rate in benzene–nitrogen solution.

controlling parameter in the diffusion process. The thin boundary layer assumption ($\delta/R \ll 1$) employed in the previous analysis by Rosner and Epstein [13] is not valid during the initial stage of bubble growing, whereas it becomes a reasonable assumption for macroscopic bubble growing. Further, macroscopic bubble growth due to mass diffusion may require more accurate treatment of the conservation equation for concentration and experimental verification, especially for the bubbles by a finite amount of liquid with a limited concentration of dissolved gases [14].

In Fig. 5, results of calculation for the case of water–nitrogen system, in which surface tension is relatively high, are presented for reference purposes. The trend is similar to that of the previous organic solution systems except that its initial development is retarded, while subsequent growth occurs more or less abruptly.

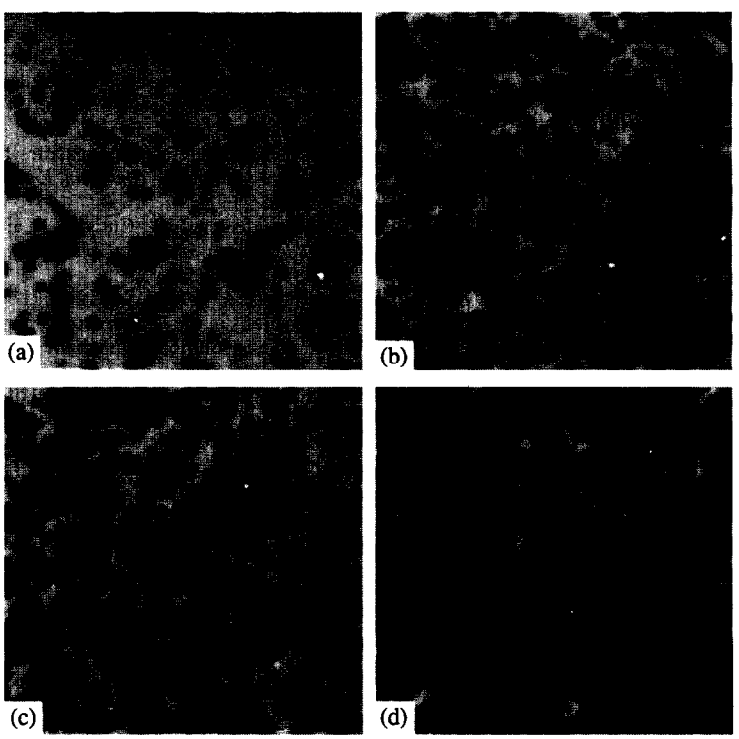

Fig. 7. The appearance of gas bubble during the late stages of decompression of benzene supersaturated with nitrogen with various initial pressures: (a) $P_i = 15$ atm; (b) 23 atm; (c) 35 atm; (d) 40 atm [7]. Photos were taken at 0.8 s after the decompression. Each frame represents an area of 2.36×2.36 mm.

Figure 6 shows the effect of varying the nucleation rate J_{nc} on the instantaneous gas to liquid volume ratio. As discussed in the previous section, J_{nc}, represents the number of critical clusters, hence gas bubble occurring per unit volume and per unit time, provided that the critical clusters do not coalesce together. Therefore, by simply multiplying J_{nc} to the known instantaneous bubble volume, one may readily obtain the total gas to liquid volume ratio at a given time. The utility of examining such variations is that, by comparing with experimental observations, one may gain some idea in determining the nucleation rate value. For reference purposes, a series of photographs taken by Hong [7], which show the appearance of gas bubble in benzene–nitrogen solution depending on the decompression amount, is shown in Fig. 7. As increasing the decompression value, the number of bubbles nucleated in unit volume, correspondingly the volume occupied by gas bubbles is shown to be increased. In fact, the nucleation rate is a parameter to predict not only the nucleation event, but also the nucleation process. This is realized in the case of evaporation at the superheat limit [30, 31] and nucleation of silicon after laser melting [32]. The time required for the appearance of macroscopic size bubble, which was observed by Hong [7] and Kaddah and Robertson [1] is in the order of seconds. These observations are also in agreement with the calculation result shown in Fig. 6. More detailed bubble growth for various cases, especially for the case that bubble growth is controlled by reaction at bubble wall, may be considered by using the phenomenological exsolution (or dissolution) rate constant [13].

CONCLUSION

The spontaneous gas bubble nucleation and subsequent bubble growth in various organic solutions initially saturated with dissolved gas have been considered in this study. A process of macroscopic bubble formation from the critical cluster has been suggested. The calculated value of the decompression amount for the homogeneous bubble nucleation and the time required for the birth of macroscopic bubble in the solutions are in reasonable agreement with observation, which validates the proposed model.

Acknowledgement—This research was partially supported by the Chung-Ang University Special Research Grants, 1997.

REFERENCES

1. El Kaddah, N. H. and Robertson, D. G. C., Homogeneous bubble nucleation of carbon monoxide bubble in iron drops. *Journal of Colloid and Interface Science*, 1977, **60,** 349–360.
2. Gent, A. N. and Tomkins, D. A., Nucleation and growth of gas bubble in elastomers. *Journal of Applied Physics*, 1969, **40,** 2520–2525.
3. Cho, W. J., Park, H. and Youn, J. R., Ultrasonic bubble nucleation in polyurethane for RIM applications. In *Cellular Polymers*, ed. V. Kumar and S. G. Advani. ASME MD-Vol. 38, 1992, pp. 15–24.
4. Bennett, P. B. and Elliot, D. H., *The Physiology and Medicine of Diving and Compressed Air Work*. Bailliere, Tindall and Cassell, London, 1969.
5. Hemmingsen, E. A., Supersaturation of gases in water. *Science*, 1970, **167,** 1493–1494.
6. Hemmingsen, E. A., Cavitation in gas-supersaturated solutions. *Journal of Applied Physics*, 1975, **46,** 213–218.
7. Hong, M. S., A study on gas bubble formation in supersaturated gas–liquid solution by decompression. Ph.D. thesis, Chonnam National University, Korea, 1985.
8. Van Stralen, S. J. D. and Cole, R., *Boiling Phenomena*. Hemisphere, New York, 1979.
9. Kwak, H. and Panton, R. L., Gas bubble formation in nonequilibrium water–gas solutions. *Journal of Chemical Physics*, 1983, **78,** 5795–5799.
10. Eley, D. D., On the solubility of gases Part I., The inert gases in water. *Transactions of the Faraday Society*, 1939, **35,** 1281–1293.
11. Scriven, L. E., On the dynamics of phase growth. *Chemical Engineering Science*, 1959, **10,** 1–13.
12. Epstein, P. S. and Plesset, M. S., On the stability of gas bubble in liquid–gas solutions. *Journal of Chemical Physics*, 1950, **18,** 1505–1509.
13. Rosner, D. E. and Epstein, P. S., Effects of interfacial kinetics, capillarity and solute diffusion on bubble growth rates in highly supersaturated liquids. *Chemical Engineering Science*, 1972, **27,** 69–88.
14. Arefmanesh, A., Advani, S. G. and Michaelides, E. E., An accurate numerical solution for mass diffusion-induced bubble growth in viscous liquids containing limited dissolved gas. *International Journal of Heat and Mass Transfer*, 1992, **35,** 1711–1722.
15. Kwak, H. and Oh, S., Gas–vapor bubble formation—a unified approach. In *Proceedings of 25th ASME/AIChE National Heat Transfer Conference*, HTD-Vol. 96, 1988.
16. Frenkel, J., *Kinetic Theory of Liquids*. Oxford University Press, London, 1946.
17. Kwak, H. and Panton, R. L., Tensile of simple liquids predicted by a model of molecular interactions. *Journal of Physics D; Applied Physics*, 1985, **18,** 647–659.
18. Lyckman, E. W., Eckert, C. A. and Prausnitz, J. M., Generalized reference fugacities for phase equilibrium thermodynamics. *Chemical Engineering Science*, 1965, **20,** 685–691.
19. Hirschfelder, J. O., Cutis, C. F. and Bird, R. B., *Molecular Theory of Gases and Liquid*. Wiley, New York, 1954.
20. Owicki, J. C. and Scheraga, H. A., Monte-Carlo calculations in the isothermal–isobaric ensemble, 2. Dilute aqueous solution of methane. *Journal of the American Chemical Society*, 1977, **99,** 7413–7418.
21. Kwak, H. and Oh, S., A model of homogeneous bubble nucleation of CO bubble in Fe–C–O melts. Will be published in *Journal of Colloid and Interface Science*, 1997.
22. Blander, M. and Katz, J. L., Bubble nucleation in liquids. *AIChE Journal*, 1975, **21,** 833–848.
23. Defay, K. and Prigogine, I., *Surface Tension and Absorption*. Wiley, New York, 1966.
24. Kwak, H., Homogeneous bubble nucleation. *Applied Mechanics Review*, 1990, **43,** 164–165.
25. Frenkel, J., A general theory of heterophase fluctuations and pretransition phenomena. *Journal of Chemical Physics*, 1949, **7,** 538–547.
26. Kwak, H. and Yang, H., An aspect of sonoluminescence from hydrodynamic theory. *Journal of Physics Society Japan*, 1995, **64,** 1980–1992.
27. Kwak, H. and Na, J., Hydrodynamic solutions for sonoluminescing gas bubble. *Physical Review Letters*, 1996, **77,** 4454–4457.

28. Payvar, P., Mass transfer-controlled bubble growth during rapid decompression of a liquid. *International Journal of Heat and Mass Transfer*, 1987, **30,** 699–705.
29. Na, J. and Kwak, H., Characteristics of sonoluminescing gas bubble with mass transfer. *Proceedings of the KSME* 1997 *Spring Annual Meeting B*, 1997, pp. 317–322.
30. Shepherd, J. E. and Sturtevant, B., Rapid evaporation at the superheat limit. *Journal of Fluid Mechanics*, 1982, **121,** 379–402.
31. Kwak, H. and Lee, S., Homogeneous bubble nucleation predicted by a molecular interaction model. *ASME Journal of Heat Transfer*, 1991, **113,** 714–721.
32. Stiffler, S. R., Thompson, M. O. and Peercy, P. S., Supercooling nucleation of silicon after laser melting. *Physical Review Letters*, 1988, **60,** 2519–2522.